

AD-A063 994

NAVAL OCEAN SYSTEMS CENTER SAN DIEGO CA
EXACT RAY PATHS IN A MULTISEGMENT QUASIPARABOLIC IONOSPHERE. EQ--ETC(U)
SEP 78 J R HILL
NOSC/TR-300

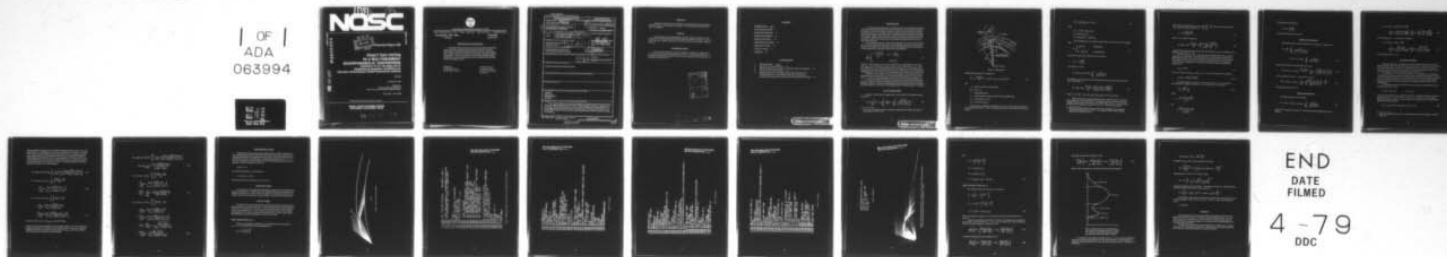
F/G 20/14

UNCLASSIFIED

NL

| OF |
ADA
063994

NOSC



END
DATE
FILMED

4-79
DDC

NOSC

NOSC TR 300

AD A063994

NOSC TR 300



Technical Report 300

EXACT RAY PATHS IN A MULTISEGMENT QUASIPARABOLIC IONOSPHERE

Equations for hf ray paths aid in
displaying propagation conditions for
real-time minicomputer-based assessment systems

JR Hill

15 September 1978

Prepared for
Naval Air Systems Command and
Naval Environmental Prediction Research Facility

June 1977 - July 1978

Approved for public release; distribution unlimited.

NAVAL OCEAN SYSTEMS CENTER
SAN DIEGO, CALIFORNIA 92152

79 01 30 074

DDC FILE COPY



NAVAL OCEAN SYSTEMS CENTER, SAN DIEGO, CA 92152

AN ACTIVITY OF THE NAVAL MATERIAL COMMAND

RR GAVAZZI, CAPT USN

Commander

HL BLOOD

Technical Director

ADMINISTRATIVE INFORMATION

This study was made for the Naval Air Systems Command (AIR 370) and the Naval Environmental Prediction Research Facility by the Naval Ocean Systems Center, EM Propagation Division (Code 532), under project MP11, as part of an effort to develop earth environment disturbance forecasting techniques. The author appreciates the help of Sean Spratt and Robert Eberhardt for computer programming, as well as Dr Henry Booker and Paul Argo for reviewing the report.

Released by
Dr JH Richter, Head
EM Propagation Division

Under authority of
JD Hightower, Head
Environmental Sciences
Department

UNCLASSIFIED

SECURITY CLASSIFICATION OF THIS PAGE (When Data Entered)

REPORT DOCUMENTATION PAGE		READ INSTRUCTIONS BEFORE COMPLETING FORM
1. REPORT NUMBER NOSC Technical Report 300 TR-300	2. GOVT ACCESSION NO.	3. RECIPIENT'S CATALOG NUMBER Technical rept.
4. TITLE (and Subtitle) EXACT RAY PATHS IN A MULTISEGMENT QUASIPARABOLIC IONOSPHERE	5. TYPE OF REPORT & PERIOD COVERED June 1977 - July 1978	
7. AUTHOR(s) JR Hill	6. PERFORMING ORG. REPORT NUMBER	
9. PERFORMING ORGANIZATION NAME AND ADDRESS Naval Ocean Systems Center San Diego, CA 92152		10. PROGRAM ELEMENT, PROJECT, TASK AREA & WORK UNIT NUMBERS 62759N, F52551, ZF52551001 MP11
11. CONTROLLING OFFICE NAME AND ADDRESS Naval Air Systems Command and Naval Environmental Prediction Research Facility		12. REPORT DATE 15 September 1978
14. MONITORING AGENCY NAME & ADDRESS (if different from Controlling Office)		13. NUMBER OF PAGES 22
15. SECURITY CLASS. (of this report) Unclassified		15a. DECLASSIFICATION/DOWNGRADING SCHEDULE
16. DISTRIBUTION STATEMENT (of this Report) Approved for public release; distribution unlimited.		
17. DISTRIBUTION STATEMENT (of the abstract entered in Block 20, if different from Report)		
18. SUPPLEMENTARY NOTES		
19. KEY WORDS (Continue on reverse side if necessary and identify by block number) Propagation Exact solution Quasiparabolic layer Ray tracing		
20. ABSTRACT (Continue on reverse side if necessary and identify by block number) Exact ray path calculations in a multiple quasiparabolic layer ionosphere are derived for use in mini- and microcomputer-based propagation assessment systems. Ionospheric profiles are modeled by quasiparabolic layers of two forms: (1) normal layers having electron density maxima and (2) valley layers having a minimum. Ray fans are displayed, demonstrating implementation of the equations on a minicomputer (SEL 810A) and a microcomputer (Tektronix 4051). The microcomputer program (in BASIC) used to calculate the single-layer propagation is included.		

DD FORM 1 JAN 73 1473

EDITION OF 1 NOV 65 IS OBSOLETE
S/N 0102-LF-014-6601

UNCLASSIFIED

SECURITY CLASSIFICATION OF THIS PAGE (When Data Entered)

393159

AB

OBJECTIVE

Improve on existing ray-tracing methods used in minicomputer-based propagation assessment systems. Two problems are addressed: (1) improvement in accuracy and (2) speed of calculations.

RESULTS

Exact ray paths can be calculated rapidly with the equations in this report. They are based on two assumptions which should be considered in their use, however. These are that (1) the earth's magnetic field and (2) any spatial variation in the ionosphere profile can be ignored.

RECOMMENDATIONS

The ray-tracing equations presented here should be considered for implementation in mini- and microcomputer-based hf assessment systems. In such implementation, the ionosphere profile should be changed for each ray hop according to known variations in the ionosphere along the hf circuit.

ACCESSION for	
NTIS	White Section <input checked="" type="checkbox"/>
DDC	Buff Section <input type="checkbox"/>
UNANNOUNCED	<input type="checkbox"/>
CLASSIFICATION	
DISTRIBUTION/AVAILABILITY CODES	
SPECIAL	
A	

CONTENTS

INTRODUCTION . . .	page 5
RAY-PATH EQUATIONS . . .	5
GROUP-PATH DISTANCE . . .	9
PHASE-PATH DISTANCE . . .	9
MULTILAYER MODEL . . .	10
DISCONNECTED LAYERS . . .	13
SAMPLE RAY PLOTS . . .	13
VALLEY LAYERS . . .	13
SUMMARY . . .	22

ILLUSTRATIONS

1. Ray-path geometry . . . page 6
2. Ray fan in a one-layer ionosphere . . . 14
3. BASIC program to produce figure 2 on a Tektronix 4051 microcomputer . . . 15
4. Ray fan in a three-layer ionosphere . . . 19
5. Multilayer model (not to scale) indicating the three different types of quasiparabolic forms: normal QP layer; valley layer; and base layer used for smooth transition to free space, with no discontinuity in the slope . . . 21

INTRODUCTION

In hf communication forecasting, it is often convenient to use simplified ionospheric models to determine the geographical coverage of radio waves. The process of determining the radio-wave path in the ionosphere is called ray tracing. Ray tracing requires computer calculations which are very extensive if the exact details of the electron density distribution and the earth's magnetic field are included. For some applications it suffices to ignore electron collisions, magnetic field effects, and precise electron density profile details. It will be convenient to assume the vertical profile to be homogeneous along the path between the transmitter and receiver.

The parabolic ionosphere is a popular approximation to the electron density distribution in both the E region and the F region. Croft and Hoogasian (reference 1) have shown that ray-path integrals can be evaluated exactly in closed form if the electron distribution is modified slightly from a parabola to what is called a quasiparabola:

$$\frac{N_e}{N_m} = \begin{cases} 1 - \frac{(r-r_m)^2 r_b^2}{y_m^2 r^2}; & r_b < r < \frac{r_m r_b}{r_b - y_m} \\ 0 & \text{(elsewhere)} \end{cases} \quad (1)$$

where N_e = electron density; N_m = maximum value of N_e ; r = radial distance from earth's center; r_m = value of r where $N_e = N_m$; r_b = value of r at layer base; and $y_m = r_m - r_b$, the layer semithickness. The quasiparabola differs from the parabola by the multiplier $(r_b/r)^2$. This factor is very nearly unity in the layer so that, for practical purposes, the quasiparabola is indistinguishable from a parabola. Its advantage arises in the solution of the ray equations.

Reference 1 gives equations for three ray-path variables: D , the distance traversed, measured along the earth's surface; P' , the group-path distance (signal transmit time multiplied by c); and P , the phase-path distance (the wave-front transmit time multiplied by c).

In this report, additional equations are presented for the ray-path coordinates along the path. General ray paths are considered, including transit through the layer or through partial layer segments. Complicated multisegmented layer profile calculations are illustrated. Ray paths trapped in a valley layer are determined along with "whispering gallery" conditions.

RAY-PATH EQUATIONS

Reference 1 shows that the integrals for D can be evaluated in the following manner (see figure 1):

$$D = 2r_0 \int_0^\theta d\theta = 2r_0 \int_{r_0}^{r_t} \frac{dr}{r \tan \theta} = 2 \int_{r_0}^{r_t} \frac{r_0^2 \cos \beta_0}{r \sqrt{r^2 \mu^2 - r_0^2 \cos^2 \beta_0}} dr \quad (2)$$

1. Croft, TA, and H Hoogasian, Exact Ray Calculations in a Quasiparabolic Ionosphere, Radio Science 3 (New Series), No 1, p 69-74, 1968.

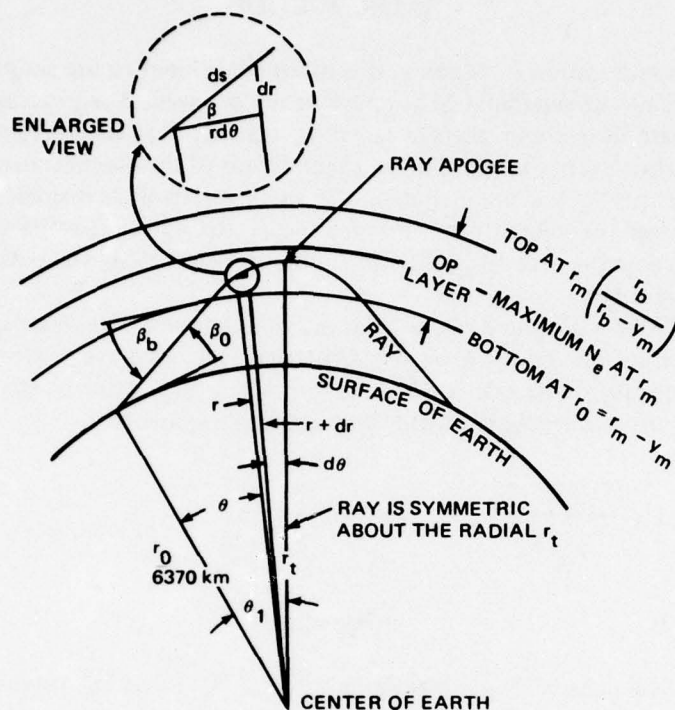


Figure 1. Ray-path geometry.

where the refractive index, μ , is defined by

$$\mu^2 \equiv 1 - \frac{80.62 N_e}{f^2} = 1 - (f_c/f)^2 + [(r_m - r)f_c r_b / (y_m f r)]^2 \quad (3)$$

and

β = angle of ray path to the horizontal

$\beta_0 = \beta$ at $r = r_0$

f = operating frequency

f_c = critical frequency of the layer ($f_c^2 = 80.62 N_m$) MKS units

r_0 = earth radius (6371 km)

r_t = r at top of ray path.

The ray path is a straight line in the region $r_0 < r < r_b$, which is free space with $\mu = 1$. In the ionospheric portion, $r > r_b$ (ie, substitution of equation 3 into equation 2), the radical becomes

$$r^2 \mu^2 - r_0^2 \cos^2 \beta_0 = Ar^2 + Br + C \quad (4)$$

with

$$A = 1 - (f_c/f)^2 + (f_c r_b / f y_m)^2$$

$$B = -2r_m (f_c r_b / f y_m)^2$$

$$C = (f_c r_b r_m / f y_m)^2 - r_0^2 \cos^2 \beta_0.$$

The coordinates (D_r , r) of a point on the ray when $r < r_b$ are on one of two straight lines

$$D_r = \begin{cases} r_0(\beta - \beta_0) & \text{(upgoing line)} \\ D - r_0(\beta - \beta_0) & \text{(downgoing line)} \end{cases} \quad (5)$$

where $\cos \beta = (r_0/r) \cos \beta_0$. When the ray is in the layer,

$$r_b < r < \frac{r_m r_b}{r_b - y_m}$$

and equation 2 becomes

$$D_r = r_0(\beta - \beta_0) + r_0^2 \cos^2 \beta_0 \int_{r_0}^r \frac{dr}{r \sqrt{Ar^2 + Br + C}}$$

The integral can be evaluated by means of standard forms given in many tables (eg, reference 2). The result is

$$D_r = r_0(\beta_b - \beta_0) + \frac{r_0^2 \cos^2 \beta_0}{\sqrt{C}} \ln \left\{ \frac{r(2C + r_b B + 2\sqrt{CX_b})}{r_b(2C + rB + 2\sqrt{CX})} \right\} \quad (6)$$

where $X = Ar^2 + Br + C$, $X_b = r_b^2 - r_0^2 \cos^2 \beta_0$, and $\beta_b = \cos^{-1}(r_0/r_b \cos \beta_0)$.

Three cases must be considered, depending on the values of f and β . If f and β are large enough, the ray will not return from the ionosphere to the ground but will proceed through to the free space above the layer. The direction taken by the ray path is indicated by the roots of the quadratic equation $Ar^2 + Br + C = 0$. If the roots are complex

2. Hill, JR, An Improved Algorithm Relating the F-Layer Peak to M(3000)F2, Union Radiologique Scientifique Internationale, Boulder, CO, 1975. Text available in NELC TN 3097, Naval Ocean Systems Center, San Diego, CA 92152.

($B^2 < 4AC$), the ray penetrates the layer. When $B^2 > 4AC$, the ray returns to the ground after reaching a maximum height, $h_t = r_t - r_0$, where

$$r_t = -\frac{B + \sqrt{B^2 - 4AC}}{2A} \quad (7)$$

When $r = r_t$, equation 6 simplifies to

$$D_t = r_0(\beta_b - \beta_0) + \frac{r_0^2 \cos \beta_0}{\sqrt{C}} \ln \left\{ \frac{(2C + Br_b + 2\sqrt{CX_b})}{r_b \sqrt{B^2 - 4AC}} \right\} \quad (8)$$

It should be noted that D_t is just half the total ray-path distance, since it corresponds to the upgoing portion. Thus, $D = 2D_t$.

The third case is $B^2 = 4AC$, which produces the so-called Pedersen ray, for which r approaches r_t asymptotically. The launch angle, β_p , of the Pedersen ray is useful since it determines the angle of a vertical cone centered at the antenna above which rays penetrate the ionosphere. An optimum antenna will beam energy below the cone to achieve best surface-to-surface communication. The Pedersen ray angle is found by calculating the maximum in r_t :

$$r_{t,\max} = -B/2A \quad (9)$$

Next, solve for β_p from $Ar_{t,\max}^2 + Br_{t,\max} + C = 0$ and C from equation 4. The result is

$$r_0 \cos \beta_p = \sqrt{-B(r_m + B/2A)/2} \quad (10)$$

D_r changes rapidly as a function of r when the ray is near r_t . It is convenient to invert equation 6 to obtain an equation for r as a function of D_r . The result is

$$r = \frac{4VC}{(V - B)^2 - 4AC} \quad (11)$$

where

$$V = \frac{2C + r_b B + 2\sqrt{CX_b}}{r_b e^u}$$

and

$$u = \frac{\sqrt{C}[D_r - r_0(\beta_b - \beta_0)]}{r_0^2 \cos \beta_0}$$

The limits on D_r are such that

$$r_b < r < \frac{r_m r_b}{r_b - y_m}$$

and can be determined by equation 6.

GROUP-PATH DISTANCE

The equation for the group-path distance can be derived in a similar manner.

$$\begin{aligned} P'_r = \int \frac{ds}{\mu} &= \int_{r_0}^r \frac{r dr}{\sqrt{r^2 \mu^2 - r_0^2 \cos^2 \beta_0}} \\ &= r_b \sin \beta_b - r_0 \sin \beta_0 + \int_{r_b}^r \frac{r dr}{\sqrt{Ar^2 + Br + C}} \end{aligned} \quad (12)$$

Again, using the tables of standard forms, the result is

$$P'_r = r_b \sin \beta_b - r_0 \sin \beta_0 + \frac{\sqrt{X} - \sqrt{X_b}}{A} + \frac{B}{2\sqrt{A^3}} \ln \left\{ \frac{\sqrt{AX_b} + Ar_b + B/2}{\sqrt{AX} + Ar + B/2} \right\} \quad (13)$$

At the ray-path peak, where $r = r_t$, equation 13 becomes

$$P'_t = r_b \sin \beta_b - r_0 \sin \beta_0 + \frac{B}{2\sqrt{A^3}} \ln \left\{ \frac{\sqrt{AX_b} + Ar_b + B/2}{-\sqrt{(B/2)^2 - AC}} \right\} - \frac{\sqrt{X_b}}{A} \quad (14)$$

The total group distance $P' = 2P'_t$.

PHASE-PATH DISTANCE

The phase path is given by the integral

$$P_r = \int \mu ds = r_b \sin \beta_b - r_0 \sin \beta_0 + \int_{r_0}^r \frac{r^2 \mu^2 dr}{r \sqrt{Ar^2 + Br + C}} \quad (15)$$

where $r^2 \mu^2$ is obtained from equation 4. The evaluation of the integral results in the equation

$$P_r = r_b \sin \beta_b - r_0 \sin \beta_0 + \sqrt{X} - \sqrt{X_b} + \frac{B}{2\sqrt{A}} \ln \frac{2Ar + B + 2\sqrt{AX}}{2Ar_b + B + 2\sqrt{AX_b}} + \frac{B r_m}{2\sqrt{C}} \ln \frac{r_b(2C + Br + 2\sqrt{CX})}{r(2C + Br_b + 2\sqrt{CX_b})} \quad (16)$$

At the ray-path peak, $r = r_t$, equation 16 simplifies to

$$P_t = r_b \sin \beta_b - r_0 \sin \beta_0 - \sqrt{X_b} + \frac{B}{2\sqrt{A}} \ln \frac{-\sqrt{B^2 - 4AC}}{2Ar_b + B + 2\sqrt{AX_b}} + \frac{B r_m}{2\sqrt{C}} \ln \frac{r_b \sqrt{B^2 - 4AC}}{2C + Br_b + 2\sqrt{CX_b}} \quad (17)$$

The total phase path is $P = 2P_t$.

MULTILAYER MODEL

During the night hours, the ionosphere is usually simple enough that a single-layer model is adequate. However, during the daytime there are two or three layers (E, F1, and F2). These can be represented by separate or connected parabolic layer segments. During the winter, the F1 layer is often better represented by a linear layer segment (reference 2). This can be accomplished by using the quasilinear segment (reference 3).

The equations 6, 13, and 16 can be written as a sum of integrals of ray properties in each layer, where the upper and lower integration limits are the altitudes (radius from earth center) of the layer intersections. The equations take one of two forms, depending on whether (1) the ray penetrates all the layers or (2) the ray is reflected in one of the layers. Models having layers separated by free-space regions will add a slight complication which will be considered later.

Let the altitude (radius) of the k^{th} layer be represented by a parabolic layer having coefficients given by 4, so that

$$X = A_k r^2 + B_k r + C_k, \quad r_k \leq r \leq r_{k+1}$$

To ensure that the electron density profile be continuous, we require that X have the same value using A_k, B_k, C_k at $r = r_{k+1}$ as using $A_{k+1}, B_{k+1}, C_{k+1}$. Usually, we are given a model defined by equation 1 with N_m, r_b , and y_m assigned. The boundaries r_k are roughly known and should be solved for using

$$(A_k - A_{k-1})r_k^2 + (B_k - B_{k-1})r_k + (C_k - C_{k-1}) = 0 \quad (18)$$

3. Weast, RC, and SM Selby, CRC Handbook of Tables for Mathematics, Chemical Rubber Co, Cleveland, Ohio, 1970.

There are solutions to equation 18, so the solution consistent with the model is to be determined and used. It is possible that no solution is consistent with the model. For example, if the E and F1 layers are modeled by some world map function, it is possible that under some conditions the solutions of equation 18 will not be in the ionosphere (N negative). These conditions must be checked for in practical applications. We now consider two sets of ray-path equations. First, rays which completely penetrate the ionosphere and second, rays which reflect from one of the layers. In case 1, we consider the path of a ray which penetrates all n layers of the model ionosphere.

$$D_r = r_0(\beta_b - \beta_0) + r_0^2 \cos \beta_0 \sum_{k=1}^n \frac{1}{\sqrt{C_k}} \ln \left\{ \frac{r_{k+1}(C_k + \sqrt{C_k X_k} + B_k r_k/2)}{r_k(C_k + \sqrt{C_k X_{k+1}} + B_k r_{k+1}/2)} \right\} \quad (19)$$

$$P'_r = r_b \sin \beta_b - r_0 \sin \beta_0 + \sum_{k=1}^n \left\{ \frac{\sqrt{X_{k+1}} - \sqrt{X_k}}{A_k} + \frac{B_k}{2\sqrt{A_k^3}} \ln \frac{A_k r_k + \sqrt{A_k X_k} + B_k/2}{A_k r_{k+1} + \sqrt{A_k X_{k+1}} + B_k/2} \right\} \quad (20)$$

$$P_r = r_b \sin \beta_b - r_0 \sin \beta_0 + \sum_{k=1}^n \left\{ \sqrt{X_{k+1}} - \sqrt{X_k} + \frac{B_k}{2\sqrt{A_k}} \ln \frac{A_k r_{k+1} + \sqrt{A_k X_{k+1}} + B_k/2}{A_k r_k + \sqrt{A_k X_k} + B_k/2} + \frac{B_k r_{m_k}}{2\sqrt{C_k}} \ln \frac{r_k(C_k + \sqrt{C_k X_{k+1}} + B_k r_{k+1}/2)}{r_{k+1}(C_k + \sqrt{C_k X_k} + B_k r_k/2)} \right\} \quad (21)$$

where $X_i = A_i r_i^2 + B_i r_i + C_i$ and r_{m_k} is r_m for the k^{th} layer.

In case 2, the ray reflects in the M^{th} layer at an altitude r_t where $X = 0$. Not only does this simplify the equation for the M^{th} layer, but it is necessary that $X = 0$ exactly. Numerical evaluation of equations 19 through 21, using equation 7 for r_{M+1} , will be inaccurate and result in square roots of negative (but small) numbers.

$$\begin{aligned}
D_r = r_0(\beta_b - \beta_0) + r_0^2 \cos \beta_0 \sum_{k=1}^{M-1} \frac{1}{\sqrt{C_k}} \ln \frac{r_{k+1}(C_k + \sqrt{C_k X_k} + B_k r_k/2)}{r_k(C_k + \sqrt{C_k X_{k+1}} + B_k r_{k+1}/2)} \\
+ r_0^2 \cos \beta_0 \frac{1}{\sqrt{C_M}} \ln \frac{2(C_M + \sqrt{C_M X_M}) + B_M r_M}{r_M \sqrt{B_M^2 - 4A_M C_M}} \quad (22)
\end{aligned}$$

$$\begin{aligned}
P'_r = r_b \sin \beta_b - r_0 \sin \beta_0 + \sum_{k=1}^{M-1} \left\{ \frac{\sqrt{X_{k+1}} - \sqrt{X_k}}{A_k} \right. \\
\left. + \frac{B_k}{2\sqrt{A_k^3}} \ln \frac{A_k r_k + \sqrt{A_k X_k} + B_k/2}{A_k r_{k+1} + \sqrt{A_k X_{k+1}} + B_k/2} \right\} \\
- \frac{\sqrt{X_M}}{A_M} + \frac{B_M}{\sqrt{A_M^3}} \ln \frac{2(A_M r_M + \sqrt{A_M X_M}) + B_M}{-\sqrt{B_M^2 - 4A_M C_M}} \quad (23)
\end{aligned}$$

$$\begin{aligned}
P_r = r_b \sin \beta_b - r_0 \sin \beta_0 + \sum_{k=1}^{M-1} \left\{ \sqrt{X_{k+1}} - \sqrt{X_k} \right. \\
+ \frac{B_k}{2\sqrt{A_k}} \ln \frac{A_k r_{k+1} + \sqrt{A_k X_{k+1}} + B_k/2}{A_k r_k + \sqrt{A_k X_k} + B_k/2} \\
\left. + \frac{B_k r_{m_k}}{2\sqrt{C_k}} \ln \frac{r_k(C_k + \sqrt{C_k X_{k+1}} + B_k r_{k+1}/2)}{r_{k+1}(C_k + \sqrt{C_k X_k} + B_k r_k/2)} \right\} \\
- \sqrt{X_M} + \frac{B_M}{2\sqrt{A_M}} \ln \frac{-\sqrt{B_M^2 - 4A_M C_M}}{2(A_M r_M + \sqrt{A_M X_M}) + B_M} \\
+ \frac{B_M r_{m_M}}{2\sqrt{C_M}} \ln \frac{r_M \sqrt{B_M^2 - 4A_M C_M}}{2(C_M + \sqrt{C_M X_M}) + B_M r_M} \quad (24)
\end{aligned}$$

DISCONNECTED LAYERS

Sometimes the layers are disconnected, which results in a "valley" between layers. This is usually the case at dawn between the E and F layers. This adds a complication requiring special treatment of the region between the upper and lower layer groups. The ray will travel in free space between the layers. Let the free space region be $r_i < r < r_{i+1}$. The sums in equations 19 through 24 will have the i^{th} layer deleted and replaced by a free-space term. For D_r in equations 19 and 22, use

$$r_0 (\beta_{i+1} - \beta_i)$$

for the i^{th} term in the sum. For P_r' and P_r , use

$$r_{i+1} \sin \beta_{i+1} - r_i \sin \beta_i$$

instead of the i^{th} terms in equations 20, 21, 23, and 24.

SAMPLE RAY PLOTS

The equations for both single-layer and multilayer models have been programmed by means of minicomputers. A sample ray plot and the BASIC program which produced it are displayed in figures 2 and 3. Figure 4 shows an example of a three-layer model and the ray-trace fan. This plot was produced on a Calcomp plotter, using an SEL-810 minicomputer.

VALLEY LAYERS

The region between layers sometimes has a smoothly varying electron density with a nonzero minimum in N , called a valley layer. It can be modeled with an inverted parabola by $d^2N/dr^2 > 0$. The minimum in N may be zero for the special base layer, used to eliminate effects of the discontinuity in N . Since the signs of some of the terms have been changed, the equations for P , P' , and D have solutions involving the arcsine function. Before listing these solutions, we rederive the constants A , B , and C for two cases.

CASE 1, BASE LAYER, $N_m = 0$

Since N_m is unavailable for scaling N_e , we use N_b defined by N_e at r_b where $r_b = r_m - y_m$. f_b is the plasma frequency corresponding to N_b .

$$N_e = N_b \left[\frac{r - r_m}{y_m} \frac{r_b}{r} \right]^2$$

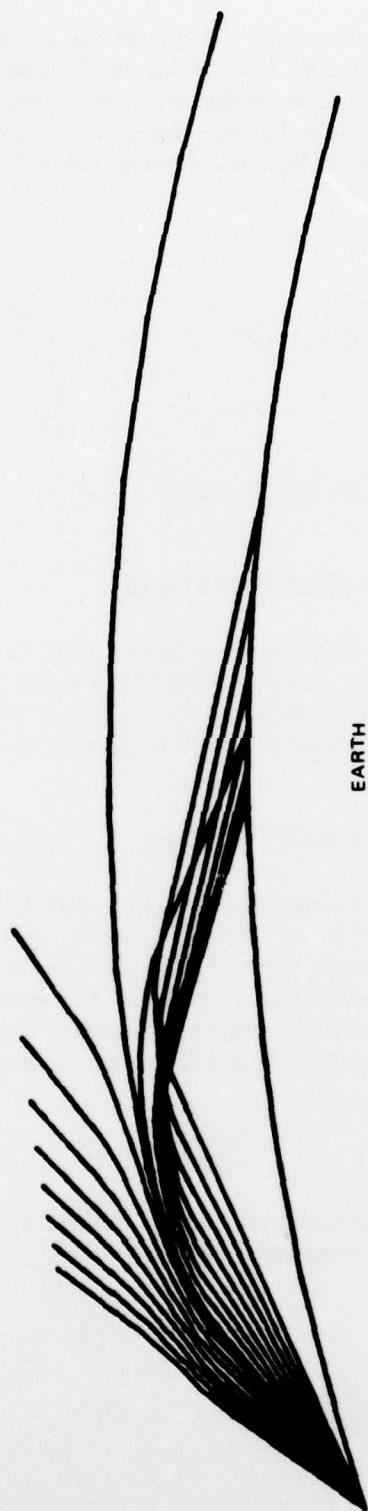


Figure 2. Ray fan in a one-layer ionosphere.


```

100 REM--RAY TRACING PROGRAM ( TEKTRONIX 4051 )
110 REM
120 REM--USES QUASI-PARABOLIC IONOSPHERE EQUATIONS
130 REM--TO DETERMINE RAY PATHS IN CLOSED FORM
140 REM
150 INIT
160 PAGE 032:
170 REM--SET UP DISPLAY PARAMETERS
180 VIEWPORT 0,130,0,90
190 WINDOW 0,3500,0,2000
200 DIM D(27),R(27),X(27),Y(27)
210 REM
220 REM NINE VARIABLES
230 REM Y1--LAYER SEMI-THICKNESS (KM)
240 REM H1--HEIGHT OF MAXIMUM ELECTRON DENSITY (KM)
250 REM B1--MINIMUM LAUNCH ANGLE (DEG)
260 REM B2--MAXIMUM LAUNCH ANGLE (DEG)
270 REM F1--OPERATING FREQUENCY (HZ)
280 REM R9--MAXIMUM RANGE OF PLOT (KM)
290 REM N1--MAXIMUM ELECTRON DENSITY (PER METER)
300 REM B7--ANGLE INCREMENT (DEG)
310 REM R7--SATELLITE HEIGHT (KM)
320 REM
330 READ Y1,H1,N1,B1,B2,B7,F1,R9,R7
340 DATA 100,300,1.0E+12,6,36,2,2.0E+7,3500,500
350 READ L,P0,D(1),C2,B3,N2,U1,U2
360 DATA 0.6371,0,0,0,25,2,13
370 R1=H1+P0
380 R2=R1-Y1
390 R6=R1*R2/(R2-Y1)
400 R7=R7+R0
410 R(1)=R0
420 R(2)=R2
430 T1=R9/(R0*2)

```

Figure 3. BASIC program used to produce figure 2 on a Tektronix 4051 microcomputer.

```

440 S1=R0*SIN(T1)
450 C1=-R0*COS(T1)
460 F2=F1/SQR(80.62*N1)
470 F3=F2*Y1
480 C3=R2*R1/F3
490 R3=R2/F3
500 A=1-1/(F2*F2)+R3*R3
510 B=-2*R1*R2*R2/(F3*F3)
520 B4=B/(2*A)
530 N2=2*U2-1
540 REM--PEDERSEN RAY ANGLE
550 B0=ACS(SQR(-B*(R1+B4)/2)/R0)
560 REM--EARTH SURFACE POINTS
570 FOR I=1 TO N2 STEP U1
580 R(I)=6371
590 S7=R9/N2-1
600 D(I)=(I-1)*S7
610 NEXT I
620 REM--MOVE TO PRINT EARTH LABEL
630 MOVE @32:1750,0
640 PRINT "HH";"EARTH";
650 GO TO 1340
660 REM--INCREMENT MINIMUM LAUNCH ANGLE UNTIL MAXIMUM
670 C2=C2+1
680 IF B3=>B2 THEN 1530
690 IF L<>U1 THEN 710
700 C2=0
710 B3=B1+C2*B7
720 B0=B3/57.29577951
730 R(1)=R0
740 D(1)=0
750 R(2)=R2
760 N2=25
770 C4=COS(B0)
780 C5=C3*C3-R0*R0*C4*C4

```

Figure 3. (Continued).

```

790 B5=B4*B4-C5*A
800 IF L<>1 THEN 820
810 B5=0
820 B8=R0*C4/R2
830 B6=ACS(B8)
840 D(2)=R0*(B6-B0) -
850 F4=R0*C4
860 K1=R2*R2-F4*F4
870 F5=R0*(B6-B0)
880 S2=R0*R0*C4/SQR(C5)
890 T2=(2*C5+R2*B+2*SQR(C5*K1))/R2
900 IF B5>0 THEN 930
910 R4=-B4
920 GO TO 940
930 R4=- (SQR(B5)+B4)
940 FOR I=1 TO V2-3 STEP V1
950 X1=(11-I)/11
960 R(I+2)=R4-(R4-R2)*X1*X1
970 K2=(A*R(I+2)+B)*R(I+2)+C5
980 D(I+2)=F5+S2*LOG(R(I+2)*T2/(2*C5+R(I+2)*B+2*SQR(C5*K2)))
990 NEXT I
1000 IF B5<>0 THEN 1020
1010 GO TO 1200
1020 IF B5<0 THEN 1130
1030 REM--REFLECTION RAY
1040 R(13)=R4
1050 D(13)=F5+S2*LOG(R(13)*T2/(2*C5+R(13)*B))
1060 FOR I=1 TO 12 STEP V1
1070 J=V2+2-I
1080 R(J)=R(I)
1090 D(J)=2*D(13)-D(I)
1100 NEXT I
1110 GO TO 1340
1120 REM--ESCAPED RAY
1130 FOR I=V2 TO N2 STEP V1

```

Figure 3. (Continued).


```

1140 FOR I=V2 TO N2 STEP V1
1150 R5=R6
1160 Y2=(N2-I)/V2
1170 R(I)=R5-(R5-R4)*Y2*Y2
1180 K2=(A*R(I)+B)*R(I)+C5
1190 D(I)=F5+S2*LOG(R(I)*T2/(2*C5+R(I)*B+2*SQR(C5*K2)))
1200 NEXT I
1210 IF R7<R6 THEN 1340
1220 N2=N2+2
1230 R(N2)=R7
1240 B9=ACS(R6*B8/R7)
1250 D(N2)=D(N2-2)+R0*(B9-B6)
1260 GO TO 1340
1270 REM--PEDERSEN RAY
1280 D1=(R9-D(11))/V2
1290 FOR I=V2 TO N2 STEP V1
1300 R(I)=-B4
1310 D(I)=D(11)+D1*(I-12)
1320 NEXT I
1330 REM--CONVERSION TO X-Y SYSTEM
1340 FOR I=1 TO N2 STEP V1
1350 X(I)=S1+R(I)*SIN(D(I)/R0-T1)
1360 IF X(I)=0 THEN 1380
1370 X(I)=0
1380 Y(I)=C1+R(I)*COS(D(I)/R0-T1)
1390 IF Y(I)=0 THEN 1410
1400 Y(I)=0
1410 NEXT I
1420 REM--MOVE TO ORIGIN
1430 MOVE #32:0,0
1440 FOR I=1 TO N2 STEP V1
1450 REM--PLOT RAY POINT
1460 DRAW #32:X(I),Y(I)
1470 NEXT I
1480 REM PLOT RAY POINT

```

Figure 3. (Continued).


```

1490 DRAW @32:X(N2),Y(N2)
1500 L=L+1
1510 IF L=1 THEN 730
1520 GO TO 670
1530 END

```

Figure 3. (Continued).



Figure 4. Ray fan in a three-layer ionosphere. The plasma frequency profile is displayed at the left side. The three layers produce three caustic surfaces, each having a "<" shape.

THIS PAGE IS BEST QUALITY PRACTICABLE
FROM COPY FURNISHED TO DDC

and

$$\begin{aligned}\mu^2 &= 1 - \left[\frac{f_b}{f} \frac{r_m - r}{y_m} \frac{r_b}{r} \right]^2 \\ A &= 1 - \left[f_b r_b / f y_m \right]^2 \\ B &= 2 r_m \left[f_b r_b / f y_m \right]^2 \\ C &= - \left[f_b r_b r_m / f y_m \right]^2 - r_0^2 \cos^2 \beta_0 .\end{aligned}\tag{25}$$

CASE 2, VALLEY LAYER, $N_m > 0$

The constants B and C are the same as in equation 25.

$$\begin{aligned}N_e &= N_m \left[1 + \frac{r - r_m}{y_m} \frac{r_b}{r} \right]^2 \\ \mu^2 &= 1 - (f_c/f)^2 - \left[\frac{f_b}{f} \frac{r_m - r}{y_m} \frac{r_b}{r} \right]^2 \\ A &= 1 - (f_c/f)^2 - \left[f_b r_b / f y_m \right]^2 .\end{aligned}\tag{26}$$

We can use Snell's law to replace $r^2 \cos^2 \beta$ by $r^2 \mu^2 \cos^2 \beta$ for studies with β known at a certain r .

Only some of the terms in equations 19, 20, and 21 are changed in the inverted QP layer solution. Let the k^{th} layer ($r_k < r < r_{k+1}$) be an inverted layer. Then the following terms in each sum are replaced. In equation 19, use

$$\frac{1}{\sqrt{-C_k}} \left\{ \arcsin \frac{B_k r_{k+1} + 2C_k}{r_{k+1} \sqrt{B_k^2 - 4A_k C_k}} - \arcsin \frac{B_k r_k + 2C_k}{r_k \sqrt{B_k^2 - 4A_k C_k}} \right\} .\tag{19i}$$

In equation 20, replace the term containing \ln with

$$\frac{B_k}{2 \sqrt{-A_k}} \left\{ \arcsin \frac{2A_k r_{k+1} + B_k}{-\sqrt{B_k^2 - 4A_k C_k}} - \arcsin \frac{2A_k r_k + B_k}{-\sqrt{B_k^2 - 4A_k C_k}} \right\} .\tag{20i}$$

And replace the last term in equation 21 with

$$\frac{B_k r_{m_k}}{2\sqrt{-C_k}} \left\{ \arcsin \frac{B_k r_{k+1} + 2C_k}{r_{k+1} \sqrt{B_k^2 - 4A_k C_k}} - \arcsin \frac{B_k r_k + 2C_k}{r_k \sqrt{B_k^2 - 4A_k C_k}} \right\}. \quad (21i)$$

Figure 5 shows an example of a multilayer profile with inverted segments.

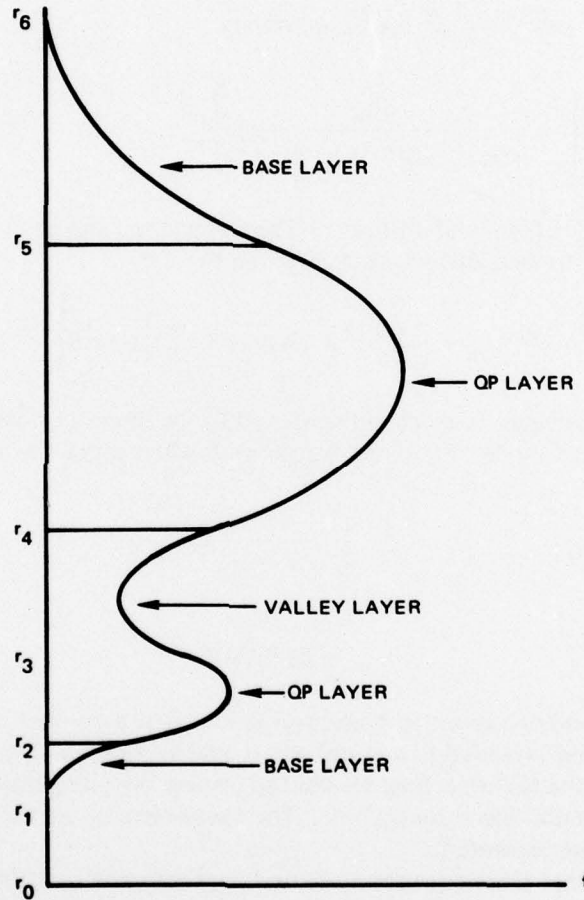


Figure 5. Multilayer model (not to scale) indicating the three different types of quasiparabolic forms: normal QP layer; valley layer; and base layer used for smooth transition to free space, with no discontinuity in the slope.

If a transmitter were located in the valley layer ($r_3 < r < r_4$), it would be possible to launch rays which are trapped between the upper and lower sides. The hop period, D_h , is obtained by substituting equation 7 for r_{k+1} and r_k in equations 19i and 19. Equation 7 can be written as

$$2Ar_t + B = B + 2C/r_t = \pm \sqrt{B^2 - 4AC} .$$

Choosing + for r_{k+1} and - for r_k in equation 19i, we have

$$D_h = \frac{2\pi r_0^2 \cos \beta_0}{\sqrt{-C_k}} = 2\pi r_0^2 \left[r_0^2 \cos^2 \beta_0 / r_0^2 \cos^2 \beta_0 - \frac{Br_m}{2} \right]^{1/2} .$$

Using Snell's law, $r^2 \cos^2 \beta = r^2 \mu^2 \cos^2 \beta$, we obtain

$$D_h = 2\pi r_0 \left\{ 1 - \left[\frac{Br_m}{2Ar^2 + B(2r + r_m)} \cos^2 \beta \right] \right\}^{-1/2}$$

where β is the angle of the ray at altitude r . The trapped ray travels in a wavelike path with period D_h and peak-to-base altitude range δr given by

$$\delta r = \frac{1}{A} \left\{ B^2 - 2ABr_m + \left[4A^2 r^2 + 2AB(2r + r_m) \right] \cos^2 \beta \right\}^{1/2} .$$

If the altitude range is small and restricted to the upper portion of the valley, we have a "whispering gallery" mode. For $\beta = 0$, we get $r = 0$ when $r = r_g$, the whispering gallery radius:

$$r_g = -B_k/2A_k .$$

SUMMARY

The quasiparabolic layer ray-tracing equations first presented in reference 1 for a single layer have been extended to a multilayer model including valley layers. The equations for points on the ray trajectory are used to display ray paths reflecting from and traversing through a multilayer ionosphere. The parameters of the whispering gallery rays in the valley layer are presented.

It is hoped that these equations will find application in multifrequency communication networks. The equations presented are compact enough so that they can be solved by means of mini- and microcomputers in an interactive manner.